Crystallization Characteristics of Calmodulin in Complex and Fused with Calcineurin Peptide†

ARTICLE *in* CRYSTAL GROWTH & DESIGN · OCTOBER 2007

Impact Factor: 4.89 · DOI: 10.1021/cg700689b

6 AUTHORS, INCLUDING:

Qilu Ye
Queen's University
22 PUBLICATIONS **390** CITATIONS
SEE PROFILE

Qun Wei
Beijing Normal University
106 PUBLICATIONS **1,047** CITATIONS
SEE PROFILE

CRYSTAL GROWTH & DESIGN
2007
VOL. 7, NO. 11
2198–2201

Crystallization Characteristics of Calmodulin in Complex and Fused with Calcineurin Peptide†

Qilu Ye,‡ Hailong Wang,§ Andrew Wong,‡ Xin Li,§ Qun Wei,§ and Zongchao Jia*,‡

Deptartment of Biochemistry, Queen's University, Kingston, Ontario K7L 3N6, Canada and Department of Biochemistry and Molecular Biology, Beijing Normal University, Beijing 100875, P.R. China

Received July 24, 2007; Revised Manuscript Received July 25, 2007

ABSTRACT: Calcineurin (CN) is the only serine/threonine protein phosphatase under the control of Ca^{2+}/calmodulin (CaM). CaM up-regulates the phosphatase activity of CN by binding to CaM-binding domain (CBD) of calcineurin subunit A. However, the disordered structure of CBD has not been resolved in all crystal structures of CN determined so far. To gain insight into the structural basis by which CaM binds to CBD of CN and exerts its interaction, we have created a fusion construction in which CBD is covalently linked to CaM via a 5-glycine flexible linker and solved the crystal structure. However, the structure that displays a novel CaM binding conformation is still debatable because of the linker between CaM and CBD and/or crystallization conditions, which may affect protein packing. To investigate whether or not the novel CaM–CBD structure could potentially represent an artifact, we have attempted cocrystallization of CaM in complex with CBD and have now obtained cocrystals in two crystal forms. Comparison of crystallization conditions, crystal morphologies, and crystal parameters indicated that both CaM in complex with CBD peptide and CaM–CBD peptide chimera have the same crystal characteristics and behaviors in crystal growth under the similar crystallization conditions. The results provide direct evidence that the glycine linker did not affect the protein structure and the crystallization conditions did not result in different conformations. The advantage of using the fusion construct includes a higher yield of the CBD peptide driven by robust expression of CaM and the ease to purify both components simultaneously.

Introduction

Calcineurin (CN) is the only calmodulin-regulated enzyme whose activation is dependent on Ca^{2+} binding to two structurally similar but functionally different Ca^{2+}-regulatory proteins: calcineurin B (CnB), an integral subunit of the enzyme, and calmodulin (CaM). The activation of CN is mediated by CAM binding to the calmodulin-binding domain (CBD) of the catalytic subunit, calcineurin A (CnA), thus inducing the displacement of an autoinhibitory domain.[8,9] In total, there are four crystal structures of CN and various complexes.[5,7,10,11] However, the CaM binding region of CnA (residues 392–468) is not visible in the electron density from all published structures, which indicates that the CaM binding region is flexible and may assume only rigid conformations upon CaM binding. The disordered structure of this region is consistent with its extreme sensitivity to proteolytic attack.[8,13] Up to now, the structure of the CaM binding region, its interaction with CaM, and the detailed understanding of activation mechanism by CaM remain unknown.

Recently, we have solved the crystal structure of calmodulin fused with the calmodulin-binding domain of calcineurin via a linker (CcL), in which a 25-residue CBD peptide (residues 389–413 of CnA) was fused to the C-terminus of calmodulin via a 5-glycine flexible linker.[22] The structure displays an unusual CaM dimer conformation in which each CaM molecule possesses a nativelike extended conformation (i.e., CaM/Ca^{2+} structure). The N-terminal lobe from one CaM and the C-terminal lobe from the second molecule form a combined binding site to trap the α-helical CBD peptide. Thus, the dimer provides two identical binding sites, each of which is similar to the conventional collapsed CaM binding conformation. This novel and unusual dimer conformation of CaM–CBD is debatable because of existence of the glycine linker between CaM and CBD peptide and possibly even crystallization conditions. More recently, we have used a recombinant CBD peptide for cocrystallization with CaM, and obtained two crystal forms that resemble the CaM–CBD chimera. The preliminary crystal data also showed that the complex is similar to the CaM–CBD chimera. These results provide direct evidence that the novel conformation of CaM–CBD is neither affected by the linker in the chimera nor by the particular crystallization conditions.

Results

The crystallization results presented here include CaM–CBD fusion and CaM–CBD complex in two crystal forms and two different space groups. The fusion construct contains CaM and the CBD peptide covalently fused through a glycine linker (termed CcL). The second form is a conventional complex crystal between CaM and the peptide obtained through cocrystallization (termed CNc). Interestingly, both CcL and CNc produced two similar crystal morphologies: hexagonal shape and plate shape (Figure 1) and two identical space groups *P*321 and *C*2 (Tables 1 and 2). CcL and CNc crystals with the same space group have almost identical unit cells. There are two molecules in the asymmetric unit in both cases. In all four crystallization conditions in which crystals were obtained, the vapor diffusion method was used at room temperature. Medium molecular weight PEGs 2000–3350 were mainly employed as precipitants. The pH was the same (pH 4.5) in all four crystallization conditions. Ammonium salt was used in three conditions except in the case of hexagonal crystals of CNc, where magnesium sulfate was used. Crystals in the ammonium salt conditions appeared at approximately 1 week and reached sufficient size for data collection in about 3 weeks. But it took 2–3 months for hexagonal crystals of CNc to reach similar size.

† Part of the special issue (Vol 7, issue 11) on the 11th International Conference on the Crystallization of Biological Macromolecules, Quebec, Canada, August 16–21, 2006 (preconference August 13–16, 2006).

* Corresponding author. Phone: 613 533 6277. Fax: 613 533 2497. E-mail: jia@queensu.ca.
‡ Queen's University.
§ Beijing Normal University.

10.1021/cg700689b CCC: $37.00
Published on Web 10/18/2007

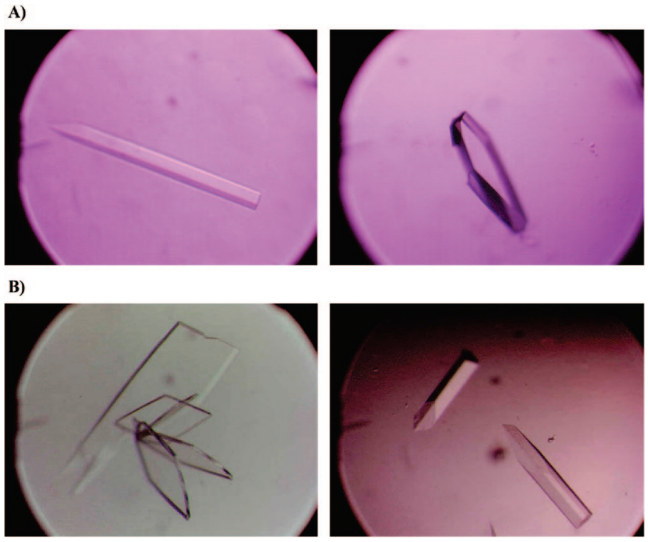

Figure 1. (A) Crystals of CNc. CBD peptide was mixed with CaM in cocrystallization. Left, *P*321; right, *C*2. (B) Crystals of CcL. Left, *C*2; right, *P*321.

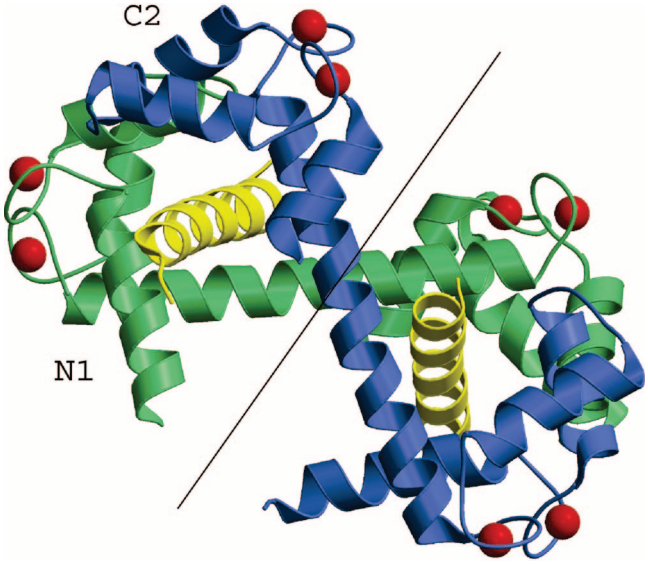

Figure 2. Overall dimer structure of CcL. The two CaM molecules in the structure are shown in green and blue. Each half of the overall structure represents a N1–*C*2 assembly, with the CBD peptide (yellow) trapped in between. Ca^{2+} ions are shown as red spheres.

Preliminary molecular replacement results show that the CNc possesses the same CcL dimer architecture that revealed a novel CaM conformation. In the dimer, each CaM molecule possesses a nativelike extended conformation and dumbbell-folding topology with maximum length of 63 Å. The N-terminal lobe from one CaM molecule and C-terminal lobe from the second molecule, conveniently described as N1–*C*2 hereon, form a combined binding site to trap the CBD peptide. Thus, the intimate homodimer provides two binding sites (Figure 2). The N1–*C*2 configuration assumes an ellipsoidal shape that closely resembles the collapsed conformation of the ligand-bound CaM, such as CaM in complex with the peptides of smooth muscle myosin light chain kinase (MLCK),[14] calmodulin-dependent protein kinase IIα,[15] and Ca^{2+}-dependent CaM kinase kinase (CaMKK).[12] The CBD peptide displays an α-helical conformation and is situated in the hydrophobic pocket generated as a result of N1–*C*2 combination. Both the N- and C-lobes in N1–*C*2 contribute a number of hydrophobic residues, including eight methionines, for the binding of the CBD peptide. These residues are exposed and form a large hydrophobic channel, similar to other collapsed CaM–ligand complexes including CaM–MLCK (Figure 3). The interaction between the peptide and the N1–*C*2 binding site of CaM is highly specific and similar to MLCK CaM binding peptide, which form a 1–8–14 hydrophobic motif.[17,20]

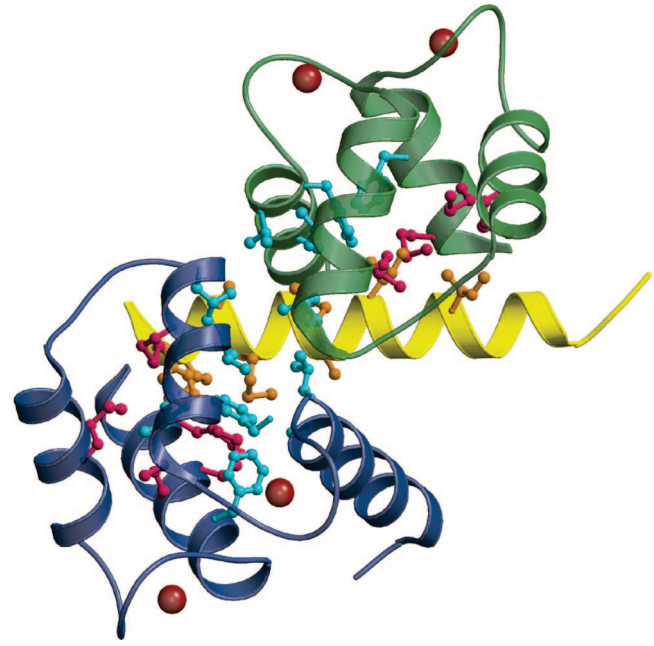

Figure 3. N1 (green) and *C*2 (blue) form a binding site. All hydrophobic residues involved in the interaction are shown. CBD peptide is in yellow. Side chains of hydrophobic residues of the peptide are in orange. Methionine residues of CaM are displayed in deep pink color and hydrophobic residues of CaM involving in binding the CBD peptide are shown in cyan color. Ca^{2+} ions are showed as red spheres.

Of the 25 residues of the CBD peptide in CcL structure, 23 residues (residues 389–411 in CnA numbering) were observed with clear electron density. The four remaining C-terminal residues of the CBD peptide and the glycine linker were not visible. This important observation clearly validates that the linker remains completely disordered and mobile. It would thus exert no restrain on the linked CBD peptide and afford the peptide with full "freedom" to interact with CaM, enabling the CcL to fully resemble the CNc structure.

Discussion

It is known that crystals occur in a great variety of shapes. The flat faces and anisotropy of crystals reflect their regular packing of molecules, atoms, or ions during the crystal growth.[4] Some specialized proteins preferentially interact with certain crystal faces. In so doing, they reduce the rate of growth in some directions and consequently change the overall crystal shape.[1] In light of the observation that CcL and CNc behave similarly in crystallization process, we can envisage that they have identical specific preferential interaction with the same crystal faces and macromolecules in the crystal growth microenvironment. Therefore, protein and peptide molecules of CcL and CNc have the same regular packing arrangement in the crystal growth microenvironment in this case, as the small linker in CcL does not interrupt protein molecule packing directions.

Table 1. Final Crystallization Conditions of CNc and CcL

	CaM complex with CBD (CNc)	CaM fusion with CBD (CcL)
hexagonal form crystals	20% PEG 3350 0.2 M magnesium formate 0.1 M Na acetate pH 4.5	29% PEG 2KMME 0.2 M ammonium sulfate 0.1 M malonic acid pH 4.5
plate form crystals	20% PEG 3350 0.2 M ammonium phosphate 0.1 M citrate acid pH 4.5	29% PEG 2KMME 0.2 M ammonium sulfate 0.1 M citrate acid pH 4.5

Table 2. Crystal Parameters of CNc and CcL

		CaM complex with CBD (CNc)	CaM fusion with CBD (CcL)
hexagonal form crystals	space group	*P*321	*P*321
	unit cell	$a = 136.94$ Å $b = 136.94$ Å $c = 46.43$ Å	$a = 137.21$ Å $b = 137.21$ Å $c = 45.28$ Å
no. of molecules in ASU		2	2
plate form crystals	space group	*C*2	*C*2
	unit cell	$a = 120.78$ Å $b = 42.62$ Å $c = 70.96$ Å $\beta = 110.18°$	$a = 121.23$ Å $b = 42.76$ Å $c = 71.15$ Å $\beta = 110.38°$
no. of molecules in ASU		2	2

The most commonly used organic and inorganic chemicals, such as PEG and ammonium salt, respectively, were used in growing both CcL and CNc crystals, further validating the notion that CcL and CNc have the same characteristics. Taken together, these results strongly support the conclusion that the novel CaM dimer conformation is not a result of either "artificial" crystallization conditions or covalent linkage.

Expression and purification of the CBD peptide is not trivial. From our experience, the best method to obtain pure CBD sample is through CaM-fusion expression followed by thrombin cleavage. However, the process was lengthy and the final yield was often not ideal for structural studies mainly because of the technical difficulties encountered in the thrombin cleavage step. On the other hand, CaM is a proven protein whose expression and purification represents a robust process. Therefore, the advantage of directly using the fusion construct without cleavage not only includes a higher yield of the CBD peptide but also the ease in purifying the peptide together with CaM simultaneously. In fact, there are many successful examples in which a glycine-rich linker is used to construct fusion proteins that facilitate protein expression and subsequent structure determination.[2,3,18]

Materials and Methods

Cloning, Protein Expression, and Purification of CcL. Cloning, expression. and purification of CcL were carried out as previously described.[22]

Protein Expression and Purification of CaM. Expression and purification of recombinant CaM were performed following the established protocol.[6,21]

CBD Peptide Preparation. A pET–CaM–CBD construct was created from an existing pET21a–CciT plasmid,[19] which contained a NotI restriction site, a continuous DNA sequence coding for CaM, a thrombin recognition site, and CnA with a *Bam*HI restriction site in order. The recombinant plasmid was transformed into *E. coli* BL21 (DE3) cells for expression. Cells from a 1 mL overnight culture were grown in 100 mL of TB medium containing ampicillin (50 μg mL^{-1}) at 37 °C. The culture was induced with 50 μM isopropyl β-D-thiogalactopyranoside (IPTG) when the OD_{600nm} of the culture reached 0.8–1.0. Following induction, the culture was incubated for about 14 h at 28 °C and then harvested. The cells were stored at −70 °C until further processing.

The cell pellet was resuspended in 10 mL of buffer (50 mM Tris-HCl pH7.6, 1 mM EDTA, 0.4 mM PMSF, 0.2% β-mercaptoethanol) and then lysed by sonication in 40 cycles of 3 s each with 30 s pulses in between cycles. The cell debris was pelleted by centrifugation for 30 min at 4 °C and 20 000 rpm. The supernatant was then heated to 85 °C for 25 min in a water bath and centrifuged for 30 min at 4 °C and 20 000 rpm. The collected supernatant was then diluted by buffer A (20 mM Tris-HCl pH 7.6, 0.2 mM PMSF, 0.2% β-mercaptoethanol) at 22 °C and adjusted to pH 7.6. The diluted supernatant was loaded onto a DEAE column pre-equilibrated with buffer A. The column was then washed with buffer A to remove unbound contaminants. Bound protein was eluted by running a linear gradient of increasing NaCl concentration using buffer A and buffer B (20 mM Tris-HCl pH 7.6, 2 M NaCl, 0.2 mM PMSF, 0.1% β-mercaptoethanol). The purity of the protein was visualized by SDS-PAGE. The pure fractions were pooled and its concentration was estimated using Bradford reagent (BioRad). The CaM tag was cleaved off by digesting with recombinant thrombin, in a ratio of 1 mg of CaM CBD to 1 unit of thrombin, at 25 °C for 24 h. The thrombin was deactivated by heating the reaction mixture to 85 °C for 25 min After the mixture was centrifuged for 30 min at 20 000 rpm, EGTA was added to the supernatant to a final concentration of 5 mM and incubated for 30 min at 22 °C. The supernatant was then diluted by buffer *C* (20mM Tris-HCl pH 7.6, 5 mM EGTA, 0.2 mM PMSF, 0.1% β-mercaptoethanol) and loaded onto a dual-column of DEAE (Pharmacia) anion-exchange and SP (Pharmacia) cation-exchange columns connected in-line, pre-equilibrated with buffer C. CBD peptide did not bind to DEAE and was washed down to the SP column with buffer C. The DEAE column was then removed, and the CBD peptide bound on the SP column eluted using a linear salt gradient from buffer C to B. The peak fractions were pooled and lyophilized and stored at −20 °C until further use.

Crystallization and Data Collection. Crystallization was performed with the hanging-drop vapor-diffusion method. The drops were prepared by mixing 1.5 μL of protein solution with 1.5 μL of reservoir solution. The CcL (8 mg/mL) and CNc (10 mg/mL, CaM:CBD peptide at 1:1 molar ratio) solutions contained 20 mM Tris-HCl, pH 7.4, and 2mM $CaCl_2$. Preliminary screening of crystallization conditions was carried out using Hampton Research screening kits. Microcrystals were obtained in the condition of 0.2 M ammonium phosphate, 20% (w/v) PEG 3350 for CNc and in condition of 0.2 M ammonium sulfate, 20% (w/v) PEG 3350 for CcL at room temperature. After several rounds of optimization, which included changing variables such as pH, protein concentration, and the type of PEG with different molecular weights, single crystals were obtained with hexagonal and plate morphology (Figure 1). The final modified crystallization conditions are listed in Table 1.

Data collection was carried out using a rotating anode X-ray source or synchrotron (Brookhaven National Laboratory) at 100 K. The crystals were cryo-protected prior to data collection. The cell parameters were determined using DNEZO.[16]

Acknowledgment. Financial support is provided by Canadian Institutes of Health Research. Z.J. is a Canada Research Chair in Structural Biology.

References

(1) Aizenberg, J.; Hanson, J.; Ilan, M.; Leiserowitz, L.; Koetzle, T. F.; Addadi, L.; Weiner, S. *FASEB J.* **1995**, *9*, 262–268.
(2) Carmichael, J. A.; Power, B. E.; Garrett, T. P.; Yazaki, P. J.; Shively, J. E.; Raubischek, A. A.; Wu, A. M.; Hudson, P. J. *J. Mol. Biol.* **2003**, *326*, 341–351.
(3) Deane, J. E.; Maher, M. J.; Langley, D. B.; Graham, S. C.; Visvader, J. E.; Guss, J. M.; Matthews, J. M. *Acta Crystallogr., Sect. D* **2003**, *59*, 1484–1486.
(4) Drenth, J. In *Principles of Protein X-ray Crystallography*; Springer-Verlag: New York, 1999; pp 10–11.
(5) Griffith, J. P.; Kim, J. L.; Kim, E. E.; Sintchak, M. D.; Thomson, J. A.; Fitzgibbon, M. J.; Fleming, M. A.; Caron, P. R.; Hsiao, K.; Navia, M. A. *Cell* **1995**, *82*, 507–522.
(6) Hayashi, N.; Matsubara, M.; Takasaki, A.; Titani, K.; Taniguchi, H. *Protein Exprressopm Purif.* **1998**, *12*, 25–28.
(7) Huai, Q.; Kim, H. Y.; Liu, Y.; Zhao, Y.; Mondragon, A.; Liu, J. O.; Ke, H. *Proc. Natl. Acad. Sci. U.S.A.* 2002,*99*, 12037–12042.
(8) Hubbard, M. J.; Klee, C. B. *Biochemistry* **1989**, *28*, 1868–1874.
(9) Ikura, M.; Clore, G. M.; Gronenborn, A. M.; Zhu, G.; Klee, C. B.; Bax, A. *Science* **1992**, *256*, 632–638.
(10) Jin, L.; Harrison, S. C. *Proc. Natl. Acad. Sci. U.S.A.* **2002**, *99*, 13522–13526.
(11) Kissinger, C. R.; Parge, H. E.; Knighton, D. R.; Lewis, C. T.; Pelletier, L. A.; Tempczyk, A.; Kalish, V. J.; Tucker, K. D.; Showalter, R. E.; Moomaw, E. W.; Gastinel, L. N.; Habuka, N.; Chen, X.; Maldonado, F.; Barker, J. E.; Bacquet, R.; Villafranca, E. *Nature* **1995**, *378*, 641–644.
(12) Kurokawa, H.; Osawa, M.; Kurihara, H.; Katayama, N.; Tokumitsu, H.; Swindells, M. B.; Kainosho, M.; Ikura, M. *J. Mol. Biol.* **2001**, *312*, 59–68.
(13) Manalan, A. S.; Klee, C. B. *Proc. Natl. Acad. Sci. U.S.A.* 1983,*80*, 4291–4295.
(14) Meador, W. E.; Means, A. R.; Quiocho, F. A. *Science* **1992**, *257*, 1251–1255.
(15) Meador, W. E.; Means, A.R., and Quiocho, F.A., *Science* **1993**, *262*, 1718–1721.
(16) Otwinowski, Z.; and Minor, W., *Methods Enzymol.* **1997**, *276*, 307–326.
(17) Rhoads, A. R.; Friedberg, F. *FASEB J.* **1997**, *11*, 331–340.
(18) Sun, S.; Geng, L.; Shamoo, Y. *Proteins* **2005**, *65*, 231–238.
(19) Wei, Q.; Lee, E. Y. *Biochem. Mol. Biol. Int.* **1997**, *41*, 169–177.
(20) Yap, K. L.; Kim, J.; Truong, K.; Sherman, M.; Yuan, T.; Ikura, M. *J. Struct. Funct. Genomics* **2000**, *1*, 8–14.
(21) Yazawa, M.; Sakuma, M.; Yagi, K. *J Biochem.* **1980**, *87*, 1313–1320.
(22) Ye, Q.; Li, X.; Wong, A.; Wei, Q.; Jia, Z *Biochemistry* **2006**, *45*, 738–745.

CG700689B